Select overexpression of Homer1a in dorsal hippocampus impairs spatial working memory

Tansu Celikel[1], Verena Marx[2,a], Florian Freudenberg[2,a], Aleksandar Zivkovic[3], Evgeny Resnik[1], Mazahir T. Hasan[4], Pawel Licznerski[2], Pavel Osten[2], Andrej Rozov[3], Peter H. Seeburg[2,*] and Martin K. Schwarz[2]

1. Department of Cell Physiology, Max-Planck Institute for Medical Research, Heidelberg, Germany
2. Department of Molecular Neurobiology, Max-Planck Institute for Medical Research, Heidelberg, Germany
3. IZN and Department of Clinical Neurobiology, University Hospital of Neurology, Heidelberg, Germany
4. Department of Biomedical Optics, Max-Planck Institute for Medical Research, Heidelberg, Germany

Review Editors: Seth Grant, Genes to Cognition Programme, The Wellcome Trust Sanger Institure UK

Henry Markram, Brain Mind Institute, Ecole Polytechnique Fédéral de Lausanne, Switzerland

Long Homer proteins forge assemblies of signaling components involved in glutamate receptor signaling in postsynaptic excitatory neurons, including those underlying synaptic transmission and plasticity. The short immediate-early gene (IEG) Homer1a can dynamically uncouple these physical associations by functional competition with long Homer isoforms. To examine the consequences of Homer1a-mediated "uncoupling" for synaptic plasticity and behavior, we generated forebrain-specific tetracycline (tet) controlled expression of Venus-tagged Homer1a (H1aV) in mice. We report that sustained overexpression of H1aV impaired spatial working but not reference memory. Most notably, a similar impairment was observed when H1aV expression was restricted to the dorsal hippocampus (HP), which identifies this structure as the principal cortical area for spatial working memory. Interestingly, H1aV overexpression also abolished maintenance of CA3-CA1 long-term potentiation (LTP). These impairments, generated by sustained high Homer1a levels, identify a requirement for long Homer forms in synaptic plasticity and temporal encoding of spatial memory.

INTRODUCTION

Immediate-early gene (IEG) activation is dynamically regulated by neural activity and suggested to be involved in synaptic plasticity and memory consolidation (Guzowski, 2002). IEGs can function as transcription factors (i.e., c-fos, *zif268*), or encode "effector" proteins (i.e., Arc, Homer1a, Ania 3), which can directly impact postsynaptic signaling mechanisms in excitatory neurons (Lanahan and Worley, 1998). Homer1a, a prominent IEG, is generated by synaptic activity-induced conversion of intronic to exonic sequence during transcription of the Homer1 gene (Bottai et al., 2002), which, unique among three Homer genes, has evolved binary expression of constitutive long (Homer1b/c) and short IEG products (Homer1a, Ania 3) (Brakeman et al., 1997). Long Homer isoforms feature an N-terminal EVH1 domain, which binds proline-rich motives in key signaling constituents of the postsynaptic spine (Naisbitt et al., 1999; Tu et al., 1998) and a C-terminal coiled-coil domain and leucine zipper for multimerization. These two domains permit long Homer proteins to physically

link postsynaptic signaling complexes. The IEG form Homer1a lacks the C-terminal coiled-coil domain and hence competes with long Homer isoforms in binding postsynaptic signaling proteins (Xiao et al., 2000). Therefore, Homer1a functions as an endogenous dominant negative regulator of synaptic signaling, and possibly of synaptic plasticity.

These unique molecular binding properties allow for clustering and functional modulation of a plethora of different binding proteins (Ango et al., 2000; Ango et al., 2001; Sala et al., 2001; Xiao et al., 2000). Thus, within multi-protein signaling complexes, Homer isoforms can influence key synaptic players as diverse as ionotropic and metabotropic glutamate receptors, transient receptor potential channels, endoplasmic reticulum Ca^{2+} release channels, Shank scaffolding proteins as well as small GTPases and cytoskeletal proteins, which put Homer proteins at the crossroad of critical intracellular signaling processes subserving experience-dependent synaptic plasticity (Duncan et al., 2005). In agreement with these observations, it has been shown that Homer1a expression is up-regulated upon a variety of experimental situations which lead to synaptic plasticity (Brakeman et al., 1997) and experience-dependent activation of sensory and hippocampal neurons (Brakeman et al., 1997; Koh et al., 2005; Nelson et al., 2004; Van Keuren-Jensen and Cline, 2006; Vazdarjanova and Guzowski, 2004; Vazdarjanova et al., 2002). Despite these findings and the presumed importance of Homer proteins for learning and memory, it is still unknown whether changes in postsynaptic levels of Homer proteins can alter synaptic plasticity and behavioral function.

We addressed these questions in transgenic mice with sustained overexpression of Venus-tagged Homer1a (H1aV) in principal neurons of the forebrain and, in a second set of experiments, in adult wild-type mice overexpressing H1aV selectively in the dorsal hippocampus (HP) from

stereotaxically delivered recombinant adeno-associated virus (rAAV). Our results demonstrate that enduring elevated Homer1a levels impair both, hippocampal long-term potentiation (LTP) expression (Hoffman et al., 2002; Mack et al., 2001; Reisel et al., 2002; Schmitt et al., 2005; Zamanillo et al., 1999) and learning to associate sensory information across time (i.e., spatial working memory), but not space (i.e., spatial reference memory) and thus identify a function for endogenous long Homer proteins in LTP and memory formation in the dorsal hippocampus.

MATERIALS AND METHODS

Generation of Homer1a transgenic mice

Rat Homer1a cDNA insert was generated by RT-PCR from rat brain RNA using primers HomVen5 5′-CGGGATCCGCGGCCGCACCATGGGGGAACAA-CCTATCTT-3′ and HomVen3 5′-CGGGATCCTTTAATCATGATTGCTGAATTG-3′, sequenced and subcloned in-frame into the BamHI site of vector pCS2, containing the coding sequence of the fluorescent protein Venus, resulting in vector pCS2-H1aV. The fused H1aV cDNA insert was excised by NotI and EcoRI and inserted into the NotI/EcoRI sites of vector pBI-5, harboring heptamerized tetracycline (tet) operator sequences flanked by two divergently oriented hCMV minimal promoters, permitting transcriptional transactivator (tTA)-dependent transcription of a luciferase gene and the H1aV gene. The resulting plasmid pBI-5/H1aV was transiently transfected into HEK293 cells together with plasmid pUHG 15-1, expressing the tet-dependent transactivator tTA under control of the CMV promoter, and tested for tet-dependent functional expression of H1aV. After functional testing, the transgene insert of pBI-5/H1aV was digested by AseI to remove vector sequences and purified by sucrose gradient. The purified DNA was microinjected in the paternal pronuclei of fertilized B6D2F1 mouse oocytes.

RNA preparation, cDNA synthesis, and RT-PCR analysis

Total RNA was isolated from total forebrain or dissected hippocampi with TRIreagent (Molecular Research Center; Cincinnati, OH) and reverse transcribed (MMLV revT; Gibco, Gaithersburg, UD) using random hexamers. Enzymes were heat-inactivated after RNAse H (USB; Cleveland, OH) treatment. RT-PCR analysis to assess ratios of mouse and rat Homer1a transcripts was carried out in a Peltier-Thermo Cycler (Watertown, MA) using primers Hom1 5′-CAACCTATCTTCAGCACTCG-3′ and Hom2 5′-AGGAGACTGAAGATCTCCTC-3′, resulting in a ∼400 bp cDNA fragment. The mixed PCR amplicons were purified (Qiagen PCR purification system; Hilden, Germany) and subsequently digested with XbaI (site located 150 bp 3′ of the rat PCR product). The relative ratio between the fragments was evaluated on an ethidium bromide-stained agarose gel. In parallel, the mixed PCR product was sequenced using primers Hom1 and Hom2 on an Applied Biosystems (Foster City, CA) capillary sequencer to compare relative peak intensities between mouse and rat transcripts.

Screening of founders via cultured ear fibroblasts

Ear fibroblasts were prepared from positive TgH1aV founders as described (Schonig and Bujard, 2003). Cells were trypsinized after reaching confluency and plated into 6-well plates divided into sets without and with doxycycline (dox, 1 g/L) (4-[Dimethlamino]-1, 4,4a,5,5a,6,11,12a-octahydro-3,5,10,12,12a-pentahydroxy-6-methyl-1,11-dioxo-2-naphthacenecarboxamide; Sigma–Aldrich, St. Louis, MO). After reaching ∼50% confluency, both the dox+ and the dox− cultures were transfected with 0.5 mg of synthetic reverse tTA (rtTA-M2s) and 0.5 mg of RL plasmids (Promega, Mannheim, Germany) using lipofectamine-2000 DNA transfection reagents as recommended by the vendor (Invitrogen Life Technologies, Carlsbad, CA). After 48 hours, cells were washed once with phosphate-buffered saline (PBS) and incubated in 0.5 ml of lysis buffer on ice. A 50 ml aliquot from each lysate was tested for FL and RL activity (Lumat LB 9581; Berthold Technologies, Wildbad, Germany). The ratio of FL to RL activity was used to correct for DNA transfection efficacy. Individual transfections and measurements were done in duplicate, usually resulting in normalized activity values that agreed within 5%. The founder showing the highest transactivation potential on ear fibroblasts (#14) was used for further analysis.

Immunohistochemistry

Adult mice (P42) were transcardially perfused with 4% PFA. Brain sections (50–100 µm) were pre-incubated in 5% normal goat serum (NGS; Sigma, St. Louis, MO) for 2 hours at room temperature and transferred to polyclonal Homer1a and GFP antibody solution containing 0.5% Triton X-100 and 1% NGS in PBS. Sections were incubated in primary antibody solution for 48 hours at 4 °C, washed 10 minutes in PBS, and incubated in biotinylated secondary antibody goat anti-rabbit IgG 1:500 (Vector; Burlingame, CA) for 2 hours at room temperature. After washing in PBS (10 minutes), the sections were incubated in streptavidin–biotinperoxidase complex (ABC standard kit, Vector) for 1–2 hours at room temperature. Immunolabeling was revealed by the glucose oxidase–diaminobenzidine (GOD-DAB) method. Vibratome sections were washed in PBS, mounted on Superfrost glass slides (Menzel; Braunschweig, Germany), dried, dehydrated, and cover-slipped with xylene.

Electrophysiology

Hippocampal slices from adult P42 wild-type and TgH1aV.Fb mice for subsequent whole-cell recordings were prepared as described previously (Hoffman et al., 2002). CA1 pyramidal neurons overexpressing H1aV were identified by a combination of fluorescent and infrared differential interference contrast videomicroscopy. Whole-cell recordings were made in current clamp mode. Stimuli (100 µs) were evoked at 0.2 Hz at an intensity adjusted to produce a single excitatory postsynaptic potential (EPSP) with an average amplitude of 2–4 mV at the beginning of recordings. EPSPs in the paired and control pathways were stimulated 0.5 seconds apart. All recordings were made at RT. The pairing protocol consisted of coincident EPSPs and postsynaptic action potentials paired five times at 100 Hz. Five paired bursts were given at 5 Hz to constitute a theta-train. Three trains (0.1 Hz) were given in total. In the unpaired controls, the postsynaptic cell was voltage-clamped to −70 mV. The amplitude of a synaptic response was calculated as the difference between the peak average of five data points, acquired a 5 kHz, in a 250-point window around the peak of the synaptic response and a 100-point average immediately preceding the stimulus. The average response of the final 5–15 minutes immediately before LTP induction was taken as the baseline, and all values were normalized to this number. In summary plots, the reported EPSPs are 1 min averages. Values are expressed as mean ± SD.

Viral gene transfer

Lentiviruses were produced as previously described (Miyoshi et al., 1998), with small modifications (Dittgen et al., 2004). Briefly, human embryonic kidney 293FT cells (Invitrogen) were transfected by using the calcium–phosphate method with three plasmids: expression vector and two helper, 8.9 and vesicular stomatitis virus G protein vectors at 1, 7.5, and 5.5 µg of DNA per 10-cm plate. After 48 hours, the supernatants of four plates were pooled, spun at 780 × g for 5 minutes, filtered at a 0.45-µm pore size, spun at 83 000 × g for 1.5 hours, and the pellet was resuspended in 100 µl of PBS. H1aV (wild-type or mutant (W24A)) was expressed from a lentiviral vector under the control of the α-CaMKII promoter, FCK(1.3)W (Dittgen et al., 2004). For stereotaxic injections of the viruses, we used standard surgical techniques (Dittgen et al., 2004). Briefly, animals were anesthetized intraperitoneally with ketamine hydrochloride (90 mg/kg)/xylazine (5 mg/kg) (Cetin et al., 2007). All pressure points and the skin incision were infused with Licain (1% lidocainhydrochlorid-1 H_2O). The stereotaxic coordinates were (from Bregma; in mm): AP, −2.6; ML, 3.6; DV, 4.0–2.5 (with five injections at 0.3 z-step).

For preparation of rAAV, the rat H1aV cDNA was subcloned into an AAV backbone containing the 480 bp human synapsin core promoter, the woodchuck post-transcriptional regulatory element (WPRE), and the bovine growth hormone polyA sequence. The same backbone carrying no cDNA was used as a control (AAV-empty). AAV pseudo-typed vectors (virions containing a 1:1 ratio of AAV1 and AAV2 capsid proteins with AAV2 ITRs) were generated as described (Kugler et al., 2003; Shevtsova et al., 2005). Shortly, human embryonic kidney 293 (HEK293) cells were transfected with the AAV cis plasmid, and the helper plasmids by standard calcium phosphate transfection. Forty-eight hours after transfection the cells were harvested and the virus purified using heparine affinity columns (Sigma, St. Louis, MO) (During et al., 2003). Purification and integrity of the viral capsid proteins (VP1-3) were monitored on a coomassie stained SDS/protein gel. The genomic titers were determined using the ABI 7700 real-time PCR cycler (Applied Biosystems) with primers designed to WPRE. For stereotaxic rAAV delivery, mice were anesthetized with intraperitoneal Ketamine/Xylazin injection. 1.5 μl of either AAV-empty or AAV-H1aV ($\sim 2 \times 10^{11}$ particles/ml) were injected bilaterally into the dorsal hippocampus (-1.8 mm from bregma, ± 1.3 mm from midline, -1.6 mm from the pia) using a custom-made stereotaxic frame. Viral particles were infused at a rate of 100 nl/min with a 10-μl syringe fitted with a 34G beveled needle by a microprocessor-controlled minipump (World Precision Instruments, FL). Behavioral training began 4 weeks after virus infusion.

Co-immunoprecipitation

Mouse brain tissues were sonicated (three times for 15 seconds each) in PBS (~ 250 mg/ml wet weight) containing 1% Triton X-100 with protease inhibitors and centrifuged for 10 min at $13\,000 \times g$. Five milliliters (1 mg) of GFP, Homer1a, Homer2, and Homer1b/c antibodies were added to 60 ml of brain tissue extract and incubated for 2 hours at 4 °C. Protein A Sepharose (60 ml, Pierce; Rockford, IL) was added for an additional hour and subsequently washed three times with PBS/Triton. Proteins were eluted in 2% SDS loading buffer. Samples were analyzed by gel electrophoresis and Western blot analysis with an mGluR1a monoclonal antibody obtained from PharMingen (San Diego, CA).

Confocal microscopy

Samples were equilibrated and embedded in Vectashield (Vector Laboratories; refractive index adjusted to 1.45 with PBS pH 7.4). The images were recorded on a LEICA SP2 AOBS confocal microscope using a 63× N.A. 1.3 objective corrected for a refractive index of 1.45. Excitation was at 514 nm, emission range was 520–600 nm.

Behavioral methods

All behavioral testing were conducted by experimenters blind to the genotype of the subjects according to the animal welfare guidelines of the Max-Planck Society. Mice were housed individually and tested during the light phase of the 12-hour light/dark cycle. Animals had *ad libitum* access to food except during training and testing on appetitively motivated tasks and during testing on unbaited tasks. During training on the appetitively motivated tasks (all excluding modified open field), animals were kept on a restricted diet aiming to keep them at 85–80% of their free-feeding weight. Animals had continous access to water in their home cages at all times.

Delayed-non-matching-to-place training

Delayed-non-matching-to-place training (also known as spatial working memory) training was studied on a T-maze as described (Reisel et al., 2002) with the exception that mice received two sessions of four trials per day for 5 days. The wooden T-maze was painted in black and elevated 150 cm from the ground. Light intensity in the three arms of the maze was 8–12 lux. The start arm (47×10 cm^2) and the two identical goal arms (35×10 cm^2) were surrounded by a 10 cm high wall. A metal food well

was located 3 cm from the end of each goal arm. Every trial of the training included two runs, sample run and choice run. On each trial, the sample arm was assigned to one of the two target arms randomly, and the mouse was directed to the sample arm where it was rewarded with 50% diluted (in water) sweetened condensed milk. About 5 seconds after the animal completed the sample run, it received the choice run, during which it was required to choose one of the two accessible arms. If the mouse chose the previously unvisited arm ("successful alternation"), it was rewarded. The numbers of correct choices out of eight daily trials were recorded.

Appetitively motivated spatial reference memory

Appetitively motivated spatial reference memory was studied on an elevated Y-maze with several extra maze cues (Figure 5A). Three identical arms (light intensity on arms: 16–30 lux) of the black wooden maze measured 50×9 cm^2 (0.5 cm beading) and were connected to each other with a triangle. Each arm of the maze was separated from the two neighboring arms by 120 degrees and equipped with a feeder placed 5 cm from the distal end. The location and orientation of the maze stayed the same throughout the training, although it was rotated in between trials to exclude the possibility that the mice identify the target arm by sensory cues unique to a particular arm. Two arms of the maze were used in a pseudorandom order as the start arm with a restriction that no arm can be assigned as start arm in more than two consecutive trials. The third arm positioned in front of a checkerboard pattern fixed to a wall was designated as target arm. On a given trial, the mouse was placed at the distal end of the start arm, facing the arm junction, allowed to run and enter arms until it found the milk. When it finished drinking the bait, it was returned to the home cage. In every trial, the number of entries to arms was recorded. Trials during which the mouse entered the target arm without first entering any other arm were designated as successful trials. To ensure that the mice did not pick the correct arm by smelling the milk, the milk was filled into the well after the mice had entered the correct arm during the last block. Mice were run in the acquisition phase of the task for 9 days and 10 trials per day. The retrieval phase of the experiment took 5 days to complete with 10 trials per day. To ensure that the mice used the spatial landmarks in the room to solve the task, we placed the apparatus in a new room at the same polar coordinates. Test sessions in the new room were like the acquisition and retrieval trials described above (Touzani et al., 2007).

Tactile spatial reference memory

Tactile spatial reference memory was studied on a T-maze identical in dimensions and material to the one used for the delayed-non-matching-to-place training. Two sets of sandpaper with different roughness and average inter-particle distance of 201 (P80) and 26 (P600) mm, covered the start and target arms (Figure 6). The target arm was randomly assigned across the trials but the target (i.e., baited) surface roughness was kept constant throughout the training. Each mouse received two training sessions (4 trials/session) per day.

Long-term retention of spatial reference memory

Long-term retention of spatial reference memory was studied after all mice reached 100% success rate during the acquisition phase of the tactile spatial reference memory task (Figure 6). The test sessions for long-term retention experiments were identical to the training sessions administered throughout the acquisition phase.

Non-baited spatial reference memory

Non-baited spatial reference memory was studied in a modified version of the open field task (modified open field). This battery of tests includes seven sessions of 6 minutes (inter-session interval ∼4 minutes) exploration in an open field with or without objects. All sessions were run in the same wooden open field measuring $60 \times 60 \times 30$ (h) cm^3, painted in black except the white colored ground. In the first session (Session 1), each mouse was run in the arena without any object. Before the next
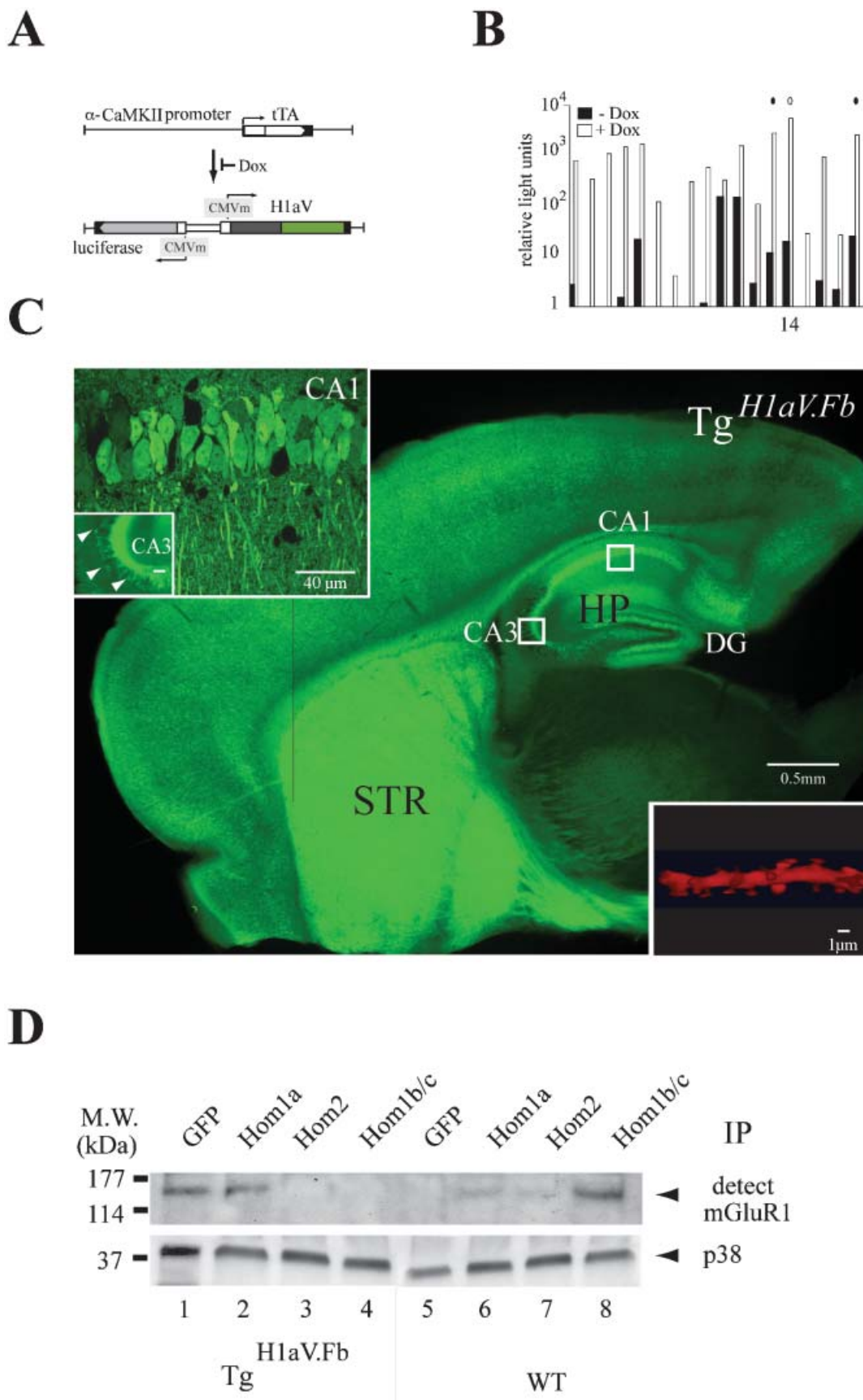
A

α-CaMKII promoter   tTA

Dox

CMVm   H1aV

luciferase   CMVm

B

■ – Dox
□ + Dox

relative light units

10^4

10^3

10^2

10

1

14

C

CA1

CA3

40 µm

Tg$^{H1aV.Fb}$

CA1

HP

CA3

DG

STR

0.5mm

1µm

D

M.W.
(kDa)   GFP   Hom1a   Hom2   Hom1b/c   GFP   Hom1a   Hom2   Hom1b/c   IP

177

114

detect
mGluR1

37

p38

1   2   3   4   5   6   7   8

H1aV.Fb

Tg   WT

Figure 1. Tetracycline-dependent forebrain expression of H1aV. (**A**) Transgenes for tet-dependent H1aV expression in the mouse forebrain. The α-CaMKII promoter directs tTA expression in forebrain principal neurons (Mayford et al., 1996). The luciferase (luc) and H1aV genes are transcribed from a bidirectional unit activated upon binding of tTA to heptamerized tet operator sequences (tetO$_7$) flanked by CMV minimal promoters. Dox prevents tTA binding to tetO$_7$,

session, five objects (see below) were placed in the arena and the mouse was habituated to the objects and their locations for three sessions (Sessions 2 to 4). To test for spatial reference memory, in Session 5, two of the objects were relocated into new positions and displaced and non-displaced object exploration was quantified. After the mouse learned the new object locations for two sessions (Sessions 5 and 6), one of the previously non-displaced objects was replaced, and the mouse was left to explore novel and habituated objects for one session. Exploration across sessions was quantified by software developed in house, written in MATLAB (Mathworks Inc., Natick, MA), running on a Pentium PC. A camera (Cohu 2200; Cohu Inc., San Diego, CA) positioned 2 meters above the arena acquired images at 25 frames/second with a spatial resolution of ~0.25 mm/pixel. After each frame is being captured, the software located the mouse in the environment and extracted the XY coordinates of the mouse by the center of mass calculation. Distance traveled between two successive frames and path traveled throughout the experiment were calculated with vector analysis. An object was classified as being explored if the mouse was within 2 cm of its periphery. Six different objects are used in these experiments: (1) a green plastic wire spool (diameter = 5 cm; length = 10 cm) with a sand paper (P400) attached to one of its sides, (2) a multi-color cross-shaped Lego® piece measuring $8.0 \times 6.5 \times 6.0$ (h) cm^3, (3) a semi-conical silicon bottle stopper with a diameter of 7.0 cm on the top and 8.2 cm at the bottom, (4) two wooden pieces glued together to form an L-shape and covered with two kinds (P80 and P140) of sand paper, (5) a Lego® construct formed into a pool with dimensions of 3.2×4.8 cm^2 (inner) and 6.4×8.0 cm^2 (outer). The construct had uneven walls; the shortest one was 3.2 and the tallest one was 6.7 cm high, and (6) a Lego® construct made of brick colored red, blue, yellow, and white, shaped into a bridge measuring $6.4 \times 3.2 \times 6.7$(h) cm^3.

RESULTS

Conditional Homer1a expression in forebrain

To regulate Homer1a expression in adult mouse forebrain, we utilized the tet-off version of the tet-dependent expression system (Gossen and Bujard, 2002; Mack et al., 2001). The rat Homer1a cDNA was fused at its 3′ end to Venus fluorescent protein cDNA (Nagai et al., 2002) and expressed from a tet-responsive bidirectional transgene harboring in addition the firefly luciferase gene (**Figure 1A**) (Baron et al., 1995; Gossen and Bujard, 2002). Expression of the luciferase gene permitted the use of ear fibroblasts in screening founders for the presence of a functional tet-responsive transcription unit (Hasan et al., 2004). The highest expresser of 18 candidate founders (**Figure 1B** and Materials and Methods) was chosen for our studies, and the corresponding transgenic line is here referred to as Tg*H1aV*.

Overexpression in forebrain was in response to α-calcium/calmodulin-dependent kinase II (α-CaMKII) promoter-driven expression of the tet-dependent tTA (Tgα-*CaMKII-tTA*) (Mayford et al., 1996) (**Figure 1A**). Double transgenic Tgα-*CaMKII-tTA*/Tg*H1aV* (abbreviated here as Tg*H1aV.Fb*) mice (studied at P42) displayed robust Venus epi-fluorescence in all forebrain structures (**Figure 1C**) (Krestel et al., 2004; Schonig and Bujard, 2003). Strong fluorescence was seen in cortical and subcortical brain regions, with homogeneous distribution in the CA1 region of the hippocampus. Antibody stainings with a Homer1a-specific antibody detected the H1aV fusion protein in fluorescent but not in non-fluorescent cells, indicating sustained expression of the IEG fusion (data not shown). Tg*H1aV.Fb* transgenic mice, when supplied with the tet derivative doxycycline in the drinking water (dox, 0.1 g/l) for 3 weeks, showed efficient down-regulation of H1aV. Thus, Tg*H1aV.Fb* mice allowed us to investigate the effect of sustained H1aV expression on hippocampal synaptic plasticity and spatial learning.

Inspection of sagittal hippocampal sections of Tg*H1aV.Fb* mice revealed intense fluorescence in the somata and dendrites of pyramidal neurons in the subiculum, the CA1 region and the dentate gyrus (**Figure 1C** and inset, upper left side). The cell bodies of CA3 neurons displayed only sparse fluorescence, as reported for other α-CaMKII promoter-driven constructs (Mack et al., 2001) (**Figure 1C** and inset, upper left side). However, robust staining was detected in CA1 pyramidal cell dendrites of stratum radiatum and oriens, mossy fiber projections from the dentate gyrus (**Figure 1C** and inset, upper left side), and dendritic spines after enlargement of a dendritic segment following deconvolution (**Figure 1C** and inset, lower right side). To quantify the proportion of H1aV expressing neurons, we counted the number of H1aV-expressing cells by direct epi-fluorescence or after staining with fluorescent or HRP conjugated antibody against Venus in randomly chosen sections of CA1 and CA3 by confocal microscopy (**Figure 1C**, white boxes). Of ~800 CA1 cells, $80 \pm 9\%$ (mean ± SD) expressed H1aV. The remaining, non-expressing 15–20% of CA1 neurons may be interneurons (Gulyas et al., 1999), indicating that the vast majority of CA1 principal cells expressed H1aV. In contrast, only ~15% of the CA3 neurons were Venus positive.

High H1aV-to-Homer1 ratio disrupts homer interaction in hippocampus

We next determined the ratio of steady-state levels of exogenous, transgenic rat H1aV transcripts *versus* those encoding the endogenous Homer1 forms in Tg*H1aV.Fb* mice. Mixed amplicons of 407 bp, generated by RT-PCR with generic Homer1 primers from either forebrain or hippocampal RNA, were sequenced to compare relative peak intensities in the 12 nucleotide positions in which the endogenous mouse sequence differs from the rat transcript. The H1aV transcripts were found to be in ~five-fold excess over all endogenous Homer1 transcripts, both in forebrain and hippocampus (data not shown). Thus, the H1aV levels in the forebrain of Tg*H1aV.Fb* mice were approximately those of Homer1a in wild-type mice after maximal electroconvulsive shock treatment (Bottai et al., 2002).

thus switching off expression of luc and H1aV transgenes. (**B**) Screening of transgenic founders for dox-dependent gene regulation. Relative light units corresponding to ratios of firefly to renilla luciferase (rlu-FL/rlu-RL) activity, measured in mouse ear fibroblast cell cultures in absence (black) and presence (white) of dox (Hasan et al., 2004), are plotted logarithmically on the Y-axis. Circles (solid and open) indicate transgenic lines selected for crossing with Tgα-*CaMKII-tTA* mice. The open circle indicates the line #14 used in this study. (**C**) Para-saggital brain section of a P42 mouse positive for both transgenes (Tg*H1aV.Fb*), in absence of dox. Robust Venus epi-fluorescence was detected in cortical and subcortical regions, especially in the striatum (STR) and the hippocampal formation (HP). Boxed regions (CA1, CA3) represent areas for quantitative H1aV expression analysis. Inset upper left: high-power confocal image of the boxed regions in CA1 and CA3. Epi-fluorescence is robust in CA1 pyramidal cell bodies and dendritic trees but sparse in CA3. Note the intense fluorescence of mossy fiber axons. Inset lower right: proximal dendritic shaft segment from a CA1 neuron after deconvolution, with the fusion-protein seen in spines. (**D**) Overexpressed H1aV fusion protein has similar binding properties as endogenous Homer1a. Representative IP-Western blot from forebrain lysates of Tg*H1aV.Fb* (N = 2) and wild-type (N = 2) P42 mice. (1), Immunoprecipitation with anti-GFP antibody pulled mGluR1 from lysates of Tg*H1aV.Fb* mice, indicating binding of H1aV to mGluR1. (2), mGluR1 was also detected with Homer1a-specific antibody. (3, 4), No association with mGluR1 was detected with antibodies against Homer2 or Homer1b/c, indicating efficient competition by overexpressed H1aV. (5), In brains of wild-type mice the GFP antibody did not pull mGluR1. (6, 7), Moderate binding was seen with antibodies against Homer1a and Homer2 in lysates of wild-type brains. (8), Antibody against Homer1b/c robustly pulled mGluR1 from lysates of wild-type brains, indicating strong association. P38 was used to show equal overall levels of protein in the lysates (OB, olfactory bulb; CTX, cerebral cortex; STR, striatum; HP, hippocampus; MW., molecular weight).
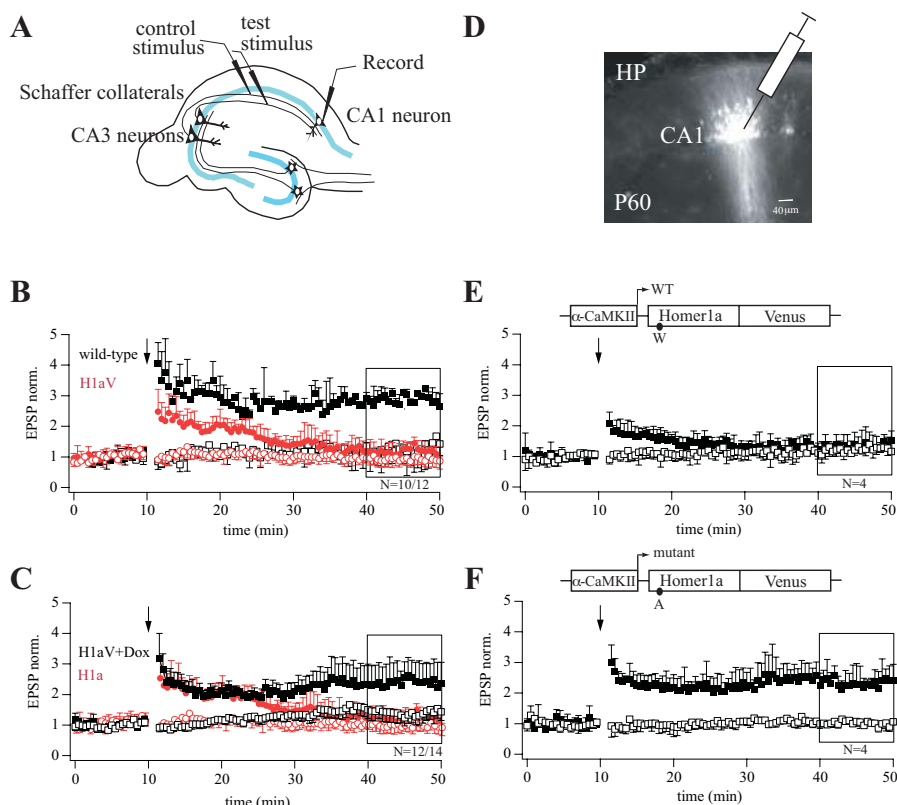
Figure 2. LTP profiles during sustained H1aV expression in CA1 pyramidal neurons. *(A) Diagram of the experimental setup for cellular LTP recordings. (B) Theta-burst pairing (TBP) induced LTP in hippocampal CA3-CA1 synapses of wild-type and TgH1aV.Fb mice. In wild-type mice, three TBP trains resulted in LTP in the paired pathway. TBP in slices from TgH1aV.Fb mice resulted in a transient potentiation of synaptic responses, lasting up to 30 minutes postpairing (red circles). TgH1aV.Fb mice completely lack the late component of TBP-induced potentiation found in wild-type mice (black squares). (C) The same protocol was applied to TgH1aV.Fb mice given dox in the drinking water from P21 until P42. Dox-treated mice (black traces), when compared to untreated ones (red traces), showed robust LTP (black squares), indicating rescue from sustained H1aV overexpression. (D) Fluorescent cells in hippocampal CA1 region 18 days after stereotaxic injection of lentivirus expressing either wild-type or mutant rat H1aV. LTP induced in hippocampal CA3-CA1 synapses of mice injected with lentivirus expressing H1aV (E) resulted in a transient potentiation of synaptic responses, whereas H1aV(W234A) expression showed normal LTP of the paired pathway (F). Schematic drawing of the lentiviral vectors illustrates LTP profiles after α-CaMKII promoter-dependent transcription of wild-type (E) and mutant (F) H1aV. The amino acid substitution in the Homer1a EVH1 domain is indicated below the expression cassette for Homer1a.*

We next questioned whether endogenous Homer proteins and H1aV share biochemical-binding characteristics, and performed immunoprecipitations for mGluR1, a primary synaptic target of Homer isoforms (de Bartolomeis and Iasevoli, 2003) (**Figure 1D**). Results revealed that the antibodies against GFP and Homer1a, but not Homer2 and Homer1b/c, precipitated mGluR1 from brain lysates of TgH1aV.Fb mice, suggesting that endogenous Homer proteins and H1aV proteins bind mGluR1 in Tg H1aV.Fb mice and that the H1aV fusion protein can compete with endogenously expressed long Homer isoforms for target binding. As expected, in immunoprecipitations from wild-type brains all antibodies, except the one directed against GFP, pulled down mGluR1 in lysates (**Figure 1D**). Our results demonstrate the ability of H1aV to interfere with endogenous Homer target–protein interactions (Tu et al., 1999; Xiao et al., 2000).

TgH1aV.Fb mice have impaired CA3-CA1 LTP

We investigated consequences of sustained H1aV expression on CA3-CA1 pyramidal cell LTP (**Figure 2A**), using the Theta-burst pairing (TBP) protocol (Hoffman et al., 2002). To induce LTP by TBP, presynaptic bursts (five stimuli at 100 Hz) of Schaffer-collateral stimulation were paired with postsynaptic current injection to initiate back-propagating action potentials. These paired bursts were repeated five times at 5 Hz to constitute a stimulation train, which was repeated three times. In

wild-type (**Figure 2B**, black filled squares), TBP generated a 2.76 ± 0.45 (mean $\pm$ SD; $N = 10$)-fold change in the EPSP amplitude in the paired pathway (test stimulus) compared to baseline, as measured 30 minutes after induction (unpaired (control) pathway 1.43 ± 0.33). In contrast, in hippocampal slices from TgH1aV.Fb mice, TBP resulted in a transient potentiation that decayed to baseline by 20–25 minutes postpairing (**Figure 2B**, paired pathway red filled circles 1.16 ± 0.11 *vs.* unpaired pathway red open circles 0.93 ± 0.06; $N = 12$). The two experimental groups also differed in their initial postsynaptic responses following TBP (WT: 4.05 ± 0.69 *vs.* TgH1aV.Fb: 2.47 ± 0.73).

To test if constitutive H1aV overexpression induces irreversible changes in synaptic efficacy, or a transient reversible effect, we switched off transgene expression for 2 weeks by adding dox (0.1 g/l) to the drinking water of P21 TgH1aV.Fb mice. As illustrated in **Figure 2C**, the superposition of normalized EPSP traces following TBP pairing in hippocampal slices from dox-treated and naïve TgH1aV.Fb mice showed that CA3-to-CA1 TBP-LTP, impaired in the naïve TgH1aV.Fb mice, was completely rescued by dox (paired pathway +dox: 2.41 ± 0.09, −dox: 2.47 ± 0.73 *versus* unpaired pathway: 1.41 ± 0.12; $N = 14$). Moreover, both, wild-type (**Figure 3A**) and TgH1aV.Fb mice (**Figure 3B**), treated at P42 with dox for 2 weeks, showed comparable levels of LTP 40 minutes after induction, indicating that sustained dox treatment does not affect LTP.
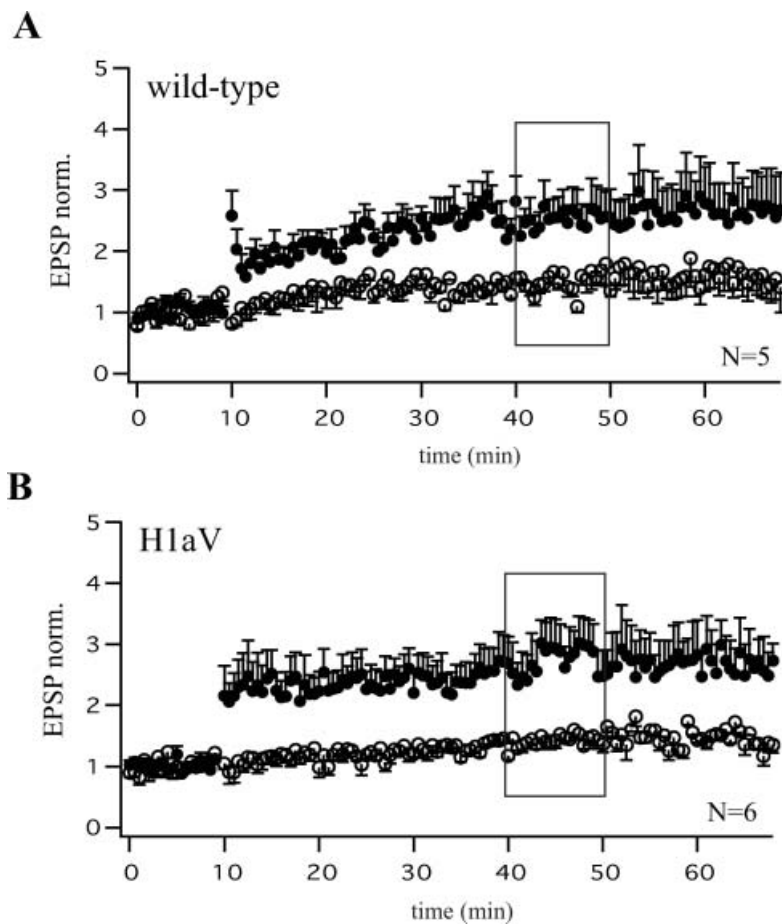
Figure 3. Comparable levels of CA3-CA1 LTP after Dox treatment of wild-type and Tg*H1aV.Fb* **mice**. *Theta-burst pairing (TBP) induced comparable levels of LTP as quantified 40 minutes after induction (black boxes* **A**, **B**) *in CA1 pyramidal cells of dox-treated wild-type (***A**, *N = 5 cells from three mice) and TgH1aV.Fb (***B**, *N = 6 cells from three mice) animals measured at P56. Both, wild-type and TgH1aV.Fb mice were supplied with dox (0.1 g/l) in the drinking water, from P42 until P56.*

To assess if loss of LTP upon H1aV overexpression was due to EVH1 domain-mediated binding of H1aV, we stereotaxically injected recombinant lentivirus expressing either a point-mutated H1aV or the wild-type form in the dorsal hippocampus of mice at P42 (**Figure 2D**). The point mutation substituted a tryptophane (W) with alanine (A) in the EVH1 domain, as H1a(W24A) abolishes binding to proline-rich target sequences (Beneken et al., 2000). Robust fluorescence was detected in infected CA1 neurons 18 days postinjection (**Figure 2D**), indicating comparable expression of both H1aV forms. Subsequently, cellular LTP was measured from fluorescent and neighboring non-fluorescent cells. Lentiviral expression of wild-type H1aV resulted in a transient potentiation of postsynaptic responses that rapidly decayed with time (**Figure 2E**; paired pathway 1.29 ± 0.09 *vs.* unpaired pathway 1.22 ± 0.08; $N = 4$), analogous to the LTP decay induced in CA1 neurons of Tg*H1aV.Fb* mice (**Figure 2B**). In contrast, lentiviral expression of the mutant H1a(W24A)V version did not interfere with LTP (**Figure 2F**; paired pathway 2.44 ± 0.12 *vs.* unpaired pathway 1.02 ± 0.07; $N = 4$). Thus, loss of LTP in Tg*H1aV.Fb* mice requires an intact EVH1 domain of H1aV and does not reflect mere overexpression of the fusion protein. Non-fluorescent pyramidal neurons directly adjacent to virus-infected fluorescent ones showed no deficits in LTP ($N = 5$; data not shown).

Sustained H1aV expression disrupts working memory

To determine if impaired hippocampal LTP in Tg*H1aV.Fb* mice correlates with behavioral deficits, we trained wild-type and Tg*H1aV.Fb* mice in spa-

tial working and reference memory tasks. Spatial working memory was tested in a rewarded T-maze non-matching-to-place task (Deacon et al., 2002; Reisel et al., 2002). Each trial on this task consists of two runs, a sample run and a choice run. During the sample run, the mouse is directed to one of the two goal arms; on the subsequent choice run, it is rewarded if it chooses the previously unsampled arm (**Figure 4A**). Mice in this task have a natural tendency to alternate and enter the previously unvisited arm. Indeed, mice of both genotypes performed the task at better than chance (50%) already during the first block (wild-type = $76 \pm 6\%$ (mean $\pm$ SEM), $N = 9$; Tg*H1aV.Fb* = $65 \pm 5\%$; $N = 12$; Chi-square, $P < 0.001$), and did not differ in this training phase (unpaired *T*-test, $P = 0.14$; **Figure 4B**). Training in the task for 80 trials (4 trials/session, 2 sessions/day for 5 consecutive days), improved the performance (two-way repeated ANOVA, $F_{1,19} = 21.205$, $P < 0.001$) of wild-type (93 ± 2; paired *T*-test, $P < 0.05$) but not Tg*H1aV.Fb* mice (71 ± 5; paired *T*-test, $P = 0.27$; **Figure 4C**). At the end of the training, wild-type mice were significantly better than Tg*H1aV.Fb* mice (unpaired *T*-test, $P < 0.005$), indicating that sustained H1aV expression impairs acquisition of spatial working memory on the T-maze.

To see if this learning deficit is reversible, we treated adult, 16 week-old Tg*H1aV.Fb* mice with dox (0.1 g/l of drinking water) for 3 weeks before retesting them in the same task. Dox treatment led to the disappearance of H1aV-associated Venus fluorescence in the forebrain, including the CA1 region of the hippocampus (**Figures 5A, B, G**). Withdrawal of dox for 3 weeks after behavioral testing allowed efficient re-induction of
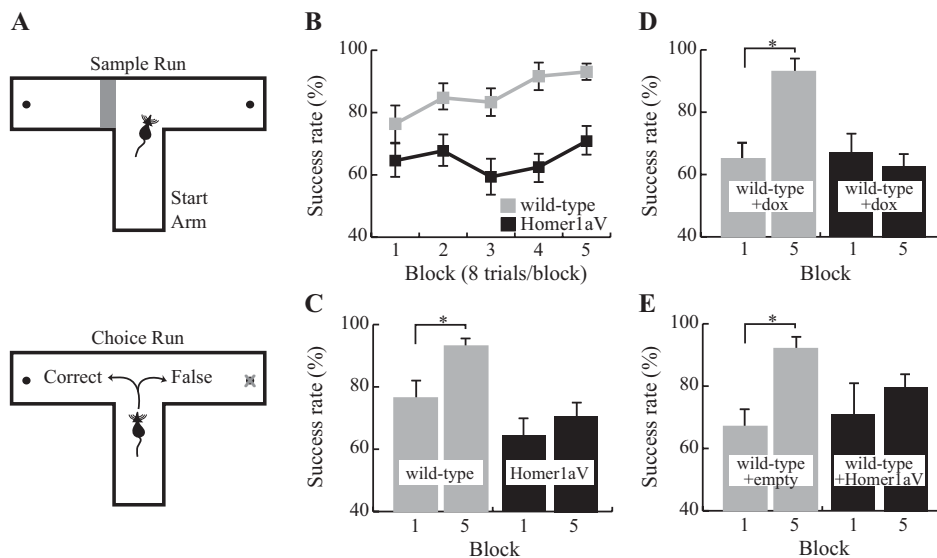
Figure 4. Impaired spatial working memory during sustained expression of Homer1a. *(A) Each trial on the delayed match to sample task, administered on a T-maze, consists of two runs. During the first (sample) run (upper panel) the mouse is forced to choose one of the two target arms by blocking the other arm. In the second (choice) run (lower panel), it is rewarded if it chooses the previously unvisited arm. (B) Wild-type (N = 9) but not TgH1aV.Fb (N = 12) learned the task. TgH1aV.Fb mice, however, showed the natural preference of rodents to visit the previously unvisited arm on this task, as shown by significantly better than chance level (50%) of spontaneous alternation during the first training block. (C) The success rate of wild-type increased over the course of the training. TgH1aV.Fb mice, however, started and finished the training at the same success rate without any significant learning throughout the training. (D) To question if the working memory deficit can be recovered upon reversal of the transgenic expression in the adult animal, we tested the wild-type (N = 7) and TgH1aV.Fb mice (N = 7) after giving dox for 4 weeks, starting 4 months after birth, and tested them on the T-maze. After five blocks of training, wild-type but not TgH1aV.Fb mice learned the task. (E) To study if the Homer1a expression in hippocampus alone could cause the working memory deficit, we virally expressed H1aV in hippocampi of adult wild-type mice for 4 weeks before testing the mice on the T-maze. Mice injected with an empty viral construct (N = 6) learned the task just like the uninfected wild-types (gray bars). Mice expressing H1aV in the hippocampus (N = 7, black bars), however, failed to learn the task, even after five blocks of training.*
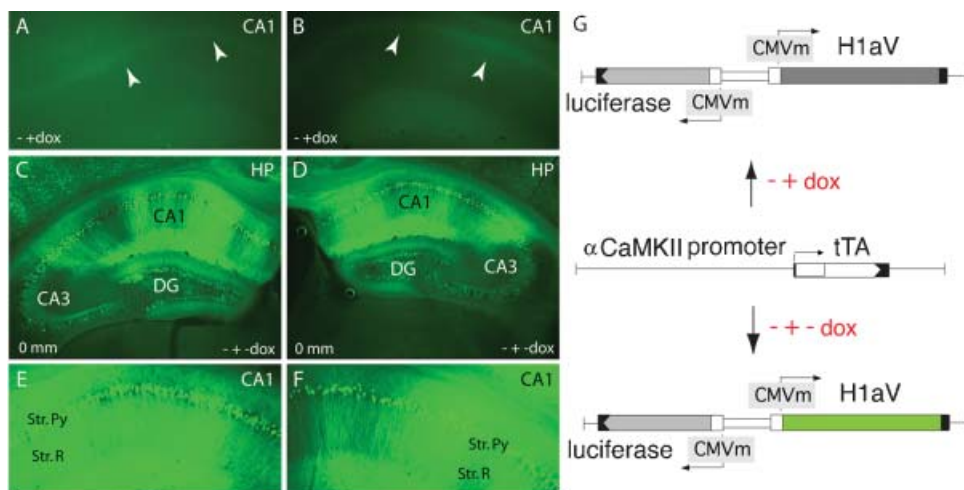

Figure 5. Tetracycline-regulated expression of *TgH1aV.Fb*. *(A, B) Representative coronal section through the CA1 region of the hippocampus (~0 mm from bregma) of a 19 week-old mouse after three weeks on dox (0.1 g/l of drinking water), demonstrating absence of GFP-enhanced H1aV fluorescence. White arrowheads point at the position of the CA1 pyramidal cell layer. − + dox indicate the chronology of dox application. (C, D) Comparable sections as in A and B, showing robust re-induction of GFP-enhanced H1aV fluorescence 3 weeks after dox withdrawal. CA1, CA2, and CA3 mark the three morphologically distinct subregions of the hippocampal pyramidal layer. Zero millimeter indicates the position from the bregma. − + − dox explains the chronology of dox application. (E, F) Magnification of the CA1 subregion shown in C, and D. Strong GFP-enhanced H1aV fluorescence was detected in both, the pyramidal cell bodies of the stratum pyramidale and in the dendrites of the stratum radiatum. (G) Schematic representation of the transgenes driving H1aV expression in the mouse forebrain. The luc and H1aV genes are expressed from a bidirectional transcription unit (upper and lower chart) activated by binding of tTa, expressed under the control of the mouse αCaMKII promoter (middle chart), to the heptamerized tet operator sequences flanked by CMV minimal promoters. Dox application can shut off transgene expression (A, B, G upper chart), which can be re-induced by withdrawal of dox (C–G, lower chart).*

H1aV expression in the hippocampus (**Figures 5C–G**), demonstrating the reversible nature of gene expression by the tet-off system.

Wild-type and Tg*H1aV.Fb* mice treated with dox (wild-type + dox, $N = 7$, and Tg*H1aV.Fb* + dox, $N = 7$; respectively) started the task with comparable success rates (block #1; wild-type + dox, $63 \pm 6.1\%$ *vs.* Tg*H1aV.Fb* + dox, $67 \pm 5.1\%$; unpaired *T*-test, $P > 0.6$; **Figure 4D**). Wild-type + dox mice learned the task gradually, reaching a success rate of $93 \pm 2.6\%$ (paired *T*-test, $P < 0.001$; block #1 *vs.* block #5). Unexpectedly, Tg*H1aV.Fb* + dox mice started and completed their training at comparably low success rates (paired *T*-test, $P > 0.59$; **Figure 4D**), indicating failure of H1aV switch-off in reversing the learning deficit.

Select expression of H1aV in adult dorsal hippocampus impairs spatial working memory

Selective lesions of the hippocampus (e.g., Reisel et al., 2002) and dorsomedial prefrontal cortex (Kellendonk et al., 2006) impair spatial working memory in the mouse. Expression of H1aV in Tg*H1aV.Fb* mice occurs in both structures. To question the role of hippocampal H1aV expression for acquisition of spatial working memory in isolation from H1aV expression in prefrontal cortex, we stereotaxically delivered rAAV expressing H1aV under the human synapsin core promoter bilaterally in the dorsal hippocampus of 16 week-old male wild-type mice. Recombinant pseudo-typed rAAV1/2 virus with preferred neuronal tropism (Burger et al., 2004; Kaplitt et al., 1994; Klugmann et al., 2005; Peel et al., 1997; Xu et al., 2001) was used for the injections. Gene expression in the hippocampus mediated by these rAAV subtypes requires 3 weeks to reach peak and persists stably for ~18 months without overt inflammation or immunogenicity (Mastakov et al., 2002; Richichi et al., 2004; Xu et al., 2001). Efficacy and spread of viral gene transfer was confirmed by immunocytochemistry on serial coronal brain sections upon completion of the behavioral experiments (**Figure 6A–D**). Histological analysis of the rAAV-injected mice 6 weeks after infusion revealed no gross abnormalities in the brain (data not shown). No GFP signal was detectable in control hippocampi having received empty rAAV (rAAV-empty, **Figure 6D**). We detected robust H1aV expression from at least 1 mm on either side of the injection point and covering the entire dorsal aspect of the hippocampus (**Figure 6A–C**). GFP fluorescence, as revealed by confocal microscopy, was found in neuronal cell bodies and dendrites in both hippocampi in the CA1-3 fields and the dentate gyrus of injected but not control mice (**Figure 6A–D**, left and right panels). Counterstaining with NeuN and counting double positive cells from representative regions showed transgene expression in ~80% of principal hippocampal CA1 neurons ($N = 600$, ~480 double positive cells), as shown for representative sections from rAAV-H1aV-injected mice (**Figure 6A–C**, right panels). The subcellular distribution of H1aV in the hippocampus was reminiscent of that in Tg*H1aV.Fb* mice (see **Figure 1C**, inset).

Selective expression of H1aV in dorsal hippocampus impaired acquisition of working memory to a similar extent as that seen in Tg*H1aV.Fb* mice. At the start of training (6 weeks postinfection), control (rAAV-empty, $N = 6$) and H1aV expressing (rAAV-H1aV, $N = 7$) mice were comparable in their success rates (block #1; rAAV-empty, $67 \pm 6.1\%$ *vs.* rAAV-H1aV, $70 \pm 10.5\%$; unpaired *T*-test, $P > 0.8$; **Figure 4E**). Control mice learned the task and reached a success rate of $92 \pm 6.2\%$ on the fifth day of training (paired *T*-test, $P < 0.05$, block#1 *vs.* block#5). rAAV-H1aV injected mice, however, failed to improve their performance significantly (Block#1 *vs.* Block#5, $70 \pm 10.5\%$ *vs.* $80 \pm 5.4\%$; paired *T*-test; $P > 0.35$), indicating that H1aV overexpression in the hippocampus could mediate the working memory deficit in Tg*H1aV.Fb* mice.

Intact reference memory in spite of sustained H1aV expression

In contrast to spatial working memory, acquisition and retention of spatial reference memory, as studied on an elevated Y-maze, a tactile reference memory paradigm and on a spontaneous exploration task, were intact in Tg*H1aV.Fb* mice. On the Y-maze, mice were trained to choose a target arm at a constant location with respect to spatial cues (**Figure 7A**).

This task requires the mice to use allocentric spatial information to locate the target arm, and hippocampal lesions impair learning on this task (Deacon et al., 2002; Reisel et al., 2002). Both genotypes learned the task at the same rate (two-way repeated measure ANOVA, $F_{1,19} = 1.67$, $P < 0.21$). At the start of the training, they performed at comparable levels (wild-type $(N = 9) = 71 \pm 5\%$, Tg*H1aV.Fb* $(N = 12) = 68 \pm 4\%$, unpaired *T*-test, $P = 0.6$) and reached similar asymptotic performance levels at the end of the training (wild-type $= 98 \pm 1\%$, Tg*H1aV.Fb* $= 100 \pm 0\%$, unpaired *T*-test, $P = 0.09$; **Figure 7B**). They did not differ in the speed of task acquisition and showed comparable increased performance across training blocks (**Figure 7C**, paired *T*-test, $P < 0.0005$), supporting the conclusion that sustained H1aV expression does not interfere with spatial reference memory as studied on the elevated Y-maze.

The two genotypes not only learned but also forgot the task at the same rate. When a subset of mice ($N = 5$ per group) was retested in the same room after 5 weeks, Tg*H1aV.Fb* and wild-type mice showed no retention of the spatial reference memory. Both groups had impaired level of success compared to the last block of the acquisition training (wild-type $= 100 \pm 0\%$ *vs.* $78 \pm 7\%$; Tg*H1aV.Fb* $= 100 \pm 0\%$ *vs.* $70 \pm 8\%$; paired *T*-test, $P < 0.05$; **Figure 7D**), similar to the first block of the acquisition (wild-type $= 80 \pm 5\%$ *vs.* $78 \pm 7\%$; Tg*H1aV.Fb* $= 76 \pm 7\%$ *vs.* 70 ± 8 %; paired *T*-test, $P > 0.5$). To ensure that mice used spatial cues in the Y-maze task, they were retested in a new room (see Materials and Methods for details) with new spatial landmarks after reaching asymptotic level of performance during the retrieval phase (**Figure 7E**). In this new room, the success rate of the animals was significantly reduced (wild-type $= 100 \pm 0\%$ *vs.* $38 \pm 5\%$; Tg*H1aV.Fb* $= 100 \pm 0\%$ *vs.* $36 \pm 5\%$; paired *T*-test, $P < 0.001$), suggesting that mice did not use intra-maze cues but relied on extra-maze spatial landmarks to solve the spatial reference memory task.

To ensure that intact reference memory in the Tg*H1aV.Fb* mice was not task specific, we further tested them on a tactile reference memory paradigm (**Figure 8A**). The apparatus was identical to the one used in the spatial working memory task on the T-maze, with the exception that the two target arms were covered with two types of sandpaper with different roughness (see Materials and Methods for details). On this task, mice were trained to associate reward location with the surface structure. Both wild-type and Tg*H1aV.Fb* mice learned the task equally ($F_{8,125} = 1.646$, $P = 0.12$; **Figure 8B**). They started the training with comparable success rates (wild-type *vs.* Tg*H1aV.Fb*; 55.7 ± 5.3 *vs.* 45.7 ± 7.2; *T*-test, $P = 0.28$) and completed the training with an average 100% success rate, suggesting that the intact spatial reference memory, as first observed in the elevated Y-maze, is not task specific, and H1aV-mediated postsynaptic signaling does not interfere with acquisition of reference memory in appetitively motivated spatial memory tasks.

Appetitive training tasks require food deprivation and extended training, which might mask cognitive impairments in recognition tasks (e.g., Zola et al., 2000). To ensure that intact spatial reference memory in Tg*H1aV.Fb* mice was not confounded by the Y-maze and tactile reference memory training protocols, we employed a hippocampus dependent spontaneous exploration task (Stupien et al., 2003; Thinus-Blanc et al., 1996). This 'modified open field' paradigm is not a learning task and does not involve reward or punishment. It includes seven sessions (Session 1–7, 6 minutes each, inter-session interval, ~4 minutes) of exploration in an open field with or without objects (see Materials and Methods). We studied the spatial reference memory after mice were habituated to five objects at constant locations for three sessions. Prior to session 5, two of the objects were repositioned, and object exploration was quantified for displaced and non-displaced objects. The behavioral response of Tg*H1aV.Fb* mice to spatial novelty was similar to that of wild-type mice. Both groups explored the objects at statistically similar rates (wild-type $= 1.01 \pm 0.33$; Tg*H1aV.Fb* $= 1.15 \pm 0.58$; unpaired *T*-test, $P > 0.85$). This result was not due to differences in
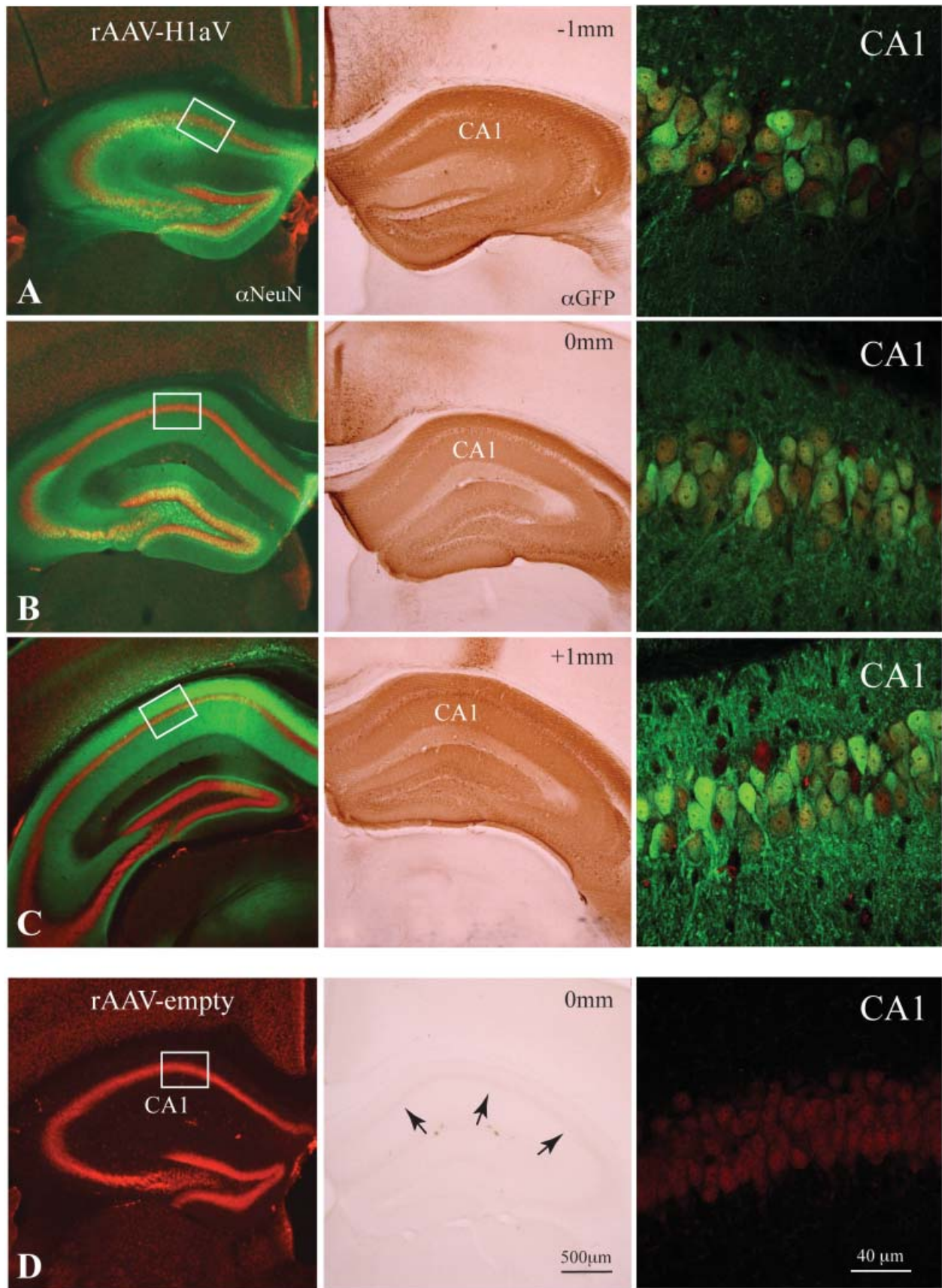
Figure 6. rAAV1/2-mediated H1aV expression in the hippocampus. *(A–D, left and middle panels) Alexa Fluor 488 or DAB enhanced anti-GFP immunohisto-chemistry for the H1aV fusion-protein on representative coronal sections approximately −1 and +1 mm from the injection site, 8 weeks after bilateral injection of rAAV1/2-H1aV/-empty. (A–D, left panels) Z-projections of the GFP-enhanced H1aV expressing green cells/neurites (oriens layer, stratum radiatum, and molecular*
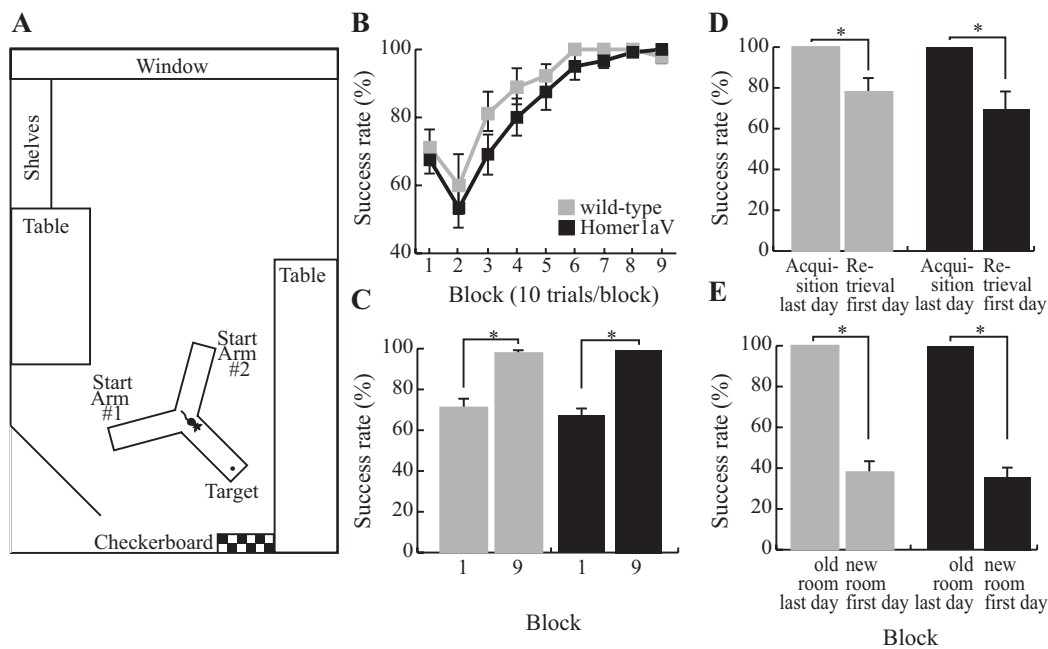
Figure 7. Sustained H1aV expression does not impair acquisition of spatial reference memory. *(A) The maze was located in a room devoted to behavioral testing of mice. In addition to spatial landmarks in the room, a checkerboard pattern was placed in front of the target arm. (B) TgH1aV.Fb mice (N = 12) did not differ from wild-type (N = 9) during task acquisition and learned the task at similar speed and rate as the wild-type. (C) Both genotypes reached an asymptotic level of performance that was significantly better than their respective performances during the first training block. (D) After a 5 weeks break from training, the mice were retested in retrieval sessions. Both genotypes showed similar reduction in performance between the last testing block of the acquisition phase and the first block of the retrieval. (E) After the mice relearned the task, they were tested in a new room to control for the spatial cue dependence of the mouse behavior. The maze was arranged in the same orientation along the poles, but this time had new landmark cues in the new location. Success rate in the new room was at chance level for both genotypes.*

motor activity (wild-type = 36.41 ± 3.42 meters/6 minutes (mean ± SD); TgH1aV.Fb = 40.07 ± 5.23 meters/6 min; $P > 0.08$), object preference ($P > 0.1$) or novel object recognition (wild-type = 1.67 ± 0.31; TgH1aV.Fb = 1.51 ± 0.46; $P > 0.8$). This result concurred with the observations on the role of Homer1a in object recognition, tested after rAAV-mediated hippocampal Homer1a expression in adult rats (Klugmann et al., 2005). Our results from elevated-Y maze, tactile reference memory paradigm and "modified open field" exploration show that, independent of training, bait, and learning condition, TgH1aV.Fb mice have intact spatial reference memory. Hence, Homer1a-mediated postsynaptic signaling does not contribute to acquisition of spatial reference memory.

Homer1a expression does not impair long-term memory

Long-term storage of memories requires IEG expression and protein synthesis. Therefore, even though sustained H1aV expression does not impair the acquisition of spatial reference memory, it is possible that it affects the long-term retention of the learned information. We tested this hypothesis on the tactile reference memory task on which both, wild-type and TgH1aV.Fb mice showed complete acquisition (**Figure 8C**). The mice were retested 3 days, 1 week, or 2 weeks after completing the acquisition

phase (**Figure 8D**). Both groups of mice had near perfect retrieval after 3 days without training (wild-type *vs.* TgH1aV.Fb; 96.4 ± 3.6 *vs.* 92.8 ± 4.6; unpaired *T*-test: $P = 0.55$). Retrieval was not significantly different from the success rates at the end of the acquisition phase of the training (wild-type, $P = 0.36$; TgH1aV.Fb, paired *T*-test: $P = 0.17$). The degree of long-term retention of the reference memory gradually decreased to 75 ± 9.4 (wild-type) and 82.1 ± 9 (TgH1aV.Fb; unpaired *T*-test: $P = 0.59$) after 1 week and 64.3 ± 7.4 (wild-type) and 71.4 ± 10.1 (TgH1aV.Fb; unpaired *T*-test: $P = 0.58$) after 2 weeks without additional training on the task. These results suggest that molecular pathways responsible for acquisition and long-term retention of spatial reference memory are not altered by sustained H1aV expression.

DISCUSSION

Numerous IEGs are rapidly activated by robust patterned synaptic activity, including sensory stimuli, seizures, LTP, and memory-related behavioral paradigms (Guzowski, 2002; Sheng and Greenberg, 1990), precluding a dissociation of the contribution of a single IEG on synaptic plasticity *in vivo*. We decided to overexpress the IEG Homer1a in a non-transient manner in principal neurons of the forebrain and, in parallel, exclusively in the dorsal

layer) on NeuN positive Cy-3 fluorescent neurons reveal transgene expression almost exclusively in the hippocampus. rAAV-empty injected brains show no GFP fluorescence antibody enhancement. (A–C, middle panels) DAB stainings of adjacent sections demonstrating robust labeling of pyramidal cell bodies in all subregions of the dorsal hippocampus. (D, middle panel) No DAB positive cells were detected in hippocampi of rAAV-empty injected mice. (A–C, right panels) High-magnification confocal dual fluorescent images (H1aV in green, NeuN in red) of representative regions from the CA1 pyramidal cell layer (marked by white boxes in A–D left panels) showing ∼80% double labeling over the total extent of the dorsal hippocampus. Note that the extent of transgene expression in the hippocampus of rAAV-infected cells is comparable with the distribution of H1aV in TgH1aV.Fb mice (Figure 1C inset). (D, right panel) No GFP fluorescence was detected in rAAV-empty infected neurons. αNeuN, anti-NeuN staining; αGFP, anti-GFP staining.
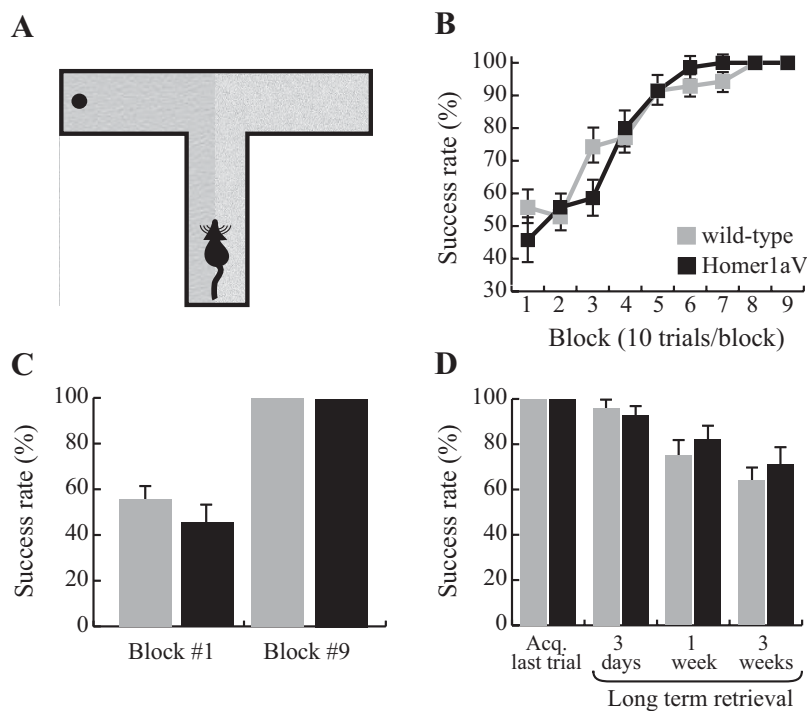
Figure 8. Intact long-term memory during sustained H1aV expression. *(A) Mice were trained on a tactile spatial reference memory task to associate the location of the food reward with one of the two sandpaper samples, before being tested in the long-term retention phase of the experiment. (B) Both wild-type (N = 7) and TgH1aV.Fb mice (N = 7) learned the task in less than 60 trials at an asymptotic performance level. (C) The overall success level across the experimental groups was not different at the start (block #1) and end (block #9) of the training. (D) After all mice reached 100% success rate, they were retested 3 days, 1 week, or 3 weeks after the end of the acquisition phase of the training. Neither group significantly differed from each other at any time point.*

hippocampus of mice, with the goal to unmask the effects of sustained Homer1a-elicited signaling on synaptic plasticity and behavior. Given that the primary function of the IEG Homer1a is to interrupt the physical linkage of postsynaptic signaling constituents forged by long-form Homer proteins, our approach revealed a critical role for the constitutively expressed long Homer proteins in hippocampal LTP expression and memory formation.

For regulatable Homer1a expression in the forebrain, we generated a tet-dependent transgenic mouse line, Tg*H1aV.Fb*, overexpressing Homer1a as a Venus fusion (H1aV) in principal forebrain neurons via transactivation from a tet-dependent transactivator protein (tTA), driven by the α-CaMKII promoter (Mayford et al., 1996). This system allowed for robust and sustained expression of H1aV in CA1 pyramidal neurons of the hippocampus and other cortical and subcortical regions in a conditional manner. The forebrain-expressed H1aV had biochemical binding properties to postsynaptic constituents similar as those of endogenous Homer1a, and its levels ($\sim$five-fold over the sum of endogenous Homer1 in hippocampus) were sufficient to compete with endogenously expressed long Homer isoforms. Intriguingly, the sustained presence of H1aV impaired maintenance of theta-pairing induced LTP in CA1 pyramidal cells. LTP maintenance was restored after suppressing H1aV expression by prolonged dox application.

To prove that the binding of H1aV to proline-rich sequence in postsynaptic interaction partners (Beneken et al., 2000) is necessary for interfering with LTP expression, we introduced a point mutation (W24A) into the EVH1 domain of H1aV, which abolishes such interactions. Expressing the H1a(W24A)V mutant by viral means in CA1 pyramidal cells did not impair LTP, strongly implying that the EVH1 domain-mediated H1aV interaction is the cause for the observed LTP impairment upon sustained H1aV expression. By contrast, viral expression of H1aV produced an LTP deficit identical to the one caused by sustained transgenic overexpression, namely transient potentiation induced by the TBP-LTP protocol with decay

to baseline after $\sim$20 minutes postpairing. Thus, Homer1a can disrupt in excitatory neurons postsynaptic signaling and plasticity mediated by the EVH1 domain of long Homer forms.

Mechanisms through which sustained H1aV expression impairs LTP maintenance are unknown but are likely to include glutamate receptor-mediated signaling pathways in postsynaptic neurons. The two classes of synaptic glutamate receptors known to interact with Homer proteins are NMDA (indirectly via Shank and PSD-95) and group I metabotropic receptors. Considering that maintenance of LTP is independent of NMDA receptors (Kullmann et al., 1992), but requires metabotropic glutamate receptors (Francesconi et al., 2004), its impairment by high H1aV levels is likely to reflect impaired downstream signaling of metabotropic glutamate receptors in the hippocampus.

Long-term changes in synaptic strength, whether they are maintained by LTP/LTD like mechanisms or others, are believed to be essential for behavioral plasticity (Lamprecht and LeDoux, 2004; Pastalkova et al., 2006; Whitlock et al., 2006). To study whether sustained H1aV expression alters behavioral functions, we trained Tg*H1aV.Fb* mice in hippocampus-dependent spatial working (i.e., delayed-non-matching-to-place) and spatial reference memory (i.e., Y-maze reference memory and tactile reference memory) tasks. Tg*H1aV.Fb* mice showed intact spatial reference memory in all tested paradigms, arguing against a task-specific rescue of reference memory. On the spatial working memory task, however, H1aV expression induced a robust deficit. These results on impaired spatial working memory and intact reference memory suggest a molecular dissociation between distinct, yet intricately linked functions of the hippocampus during spatiotemporal integration of sensory information.

Interestingly, although dox-mediated shut-off of H1aV expression completely rescued the potential to generate LTP, it failed to rescue the working memory deficit. This finding indicates that H1aV might contribute to the acquisition of spatial working memory and maintenance of LTP by distinct
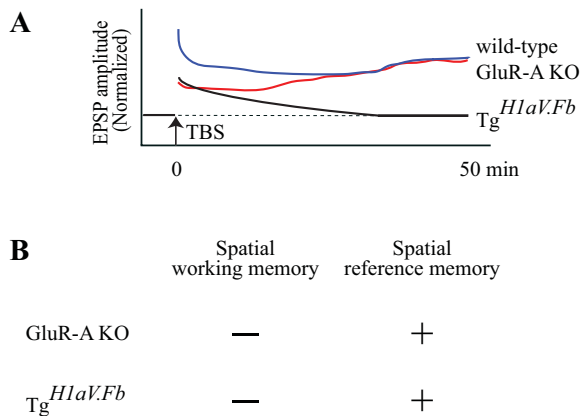
Figure 9. Maintenance of LTP after theta-burst stimulation is not required for spatial learning. *(A) Intracellular recordings from CA1 pyramidal cells show that theta-burst stimulation-induced LTP is differentially expressed in mice lacking GluR-A (GluR1) containing AMPA receptors (GluR-A KO (red trace); data from Hoffman et al. (2002)) and this report (TgH1aV.Fb, black trace). After TBP stimulation (at time 0), both GluR-A and TgH1aV.Fb mice display impaired early phase of LTP compared to wild-type mice (green trace; representative data from Hoffman et al. (2002)). In GluR-A KO, the postsynaptic responses potentiate. gradually reaching wild-type levels >25 after LTP induction. In TgH1aV.Fb mice, EPSP amplitudes decrease over time, reaching baseline level >35 min after the induction. (B) Summary of behavioral findings in GluR-A KO and TgH1aV.Fb. Both genotypes (data from Reisel et al., 2002) and current study) were impaired in T-maze, a spatial working memory task, and had intact spatial reference memory in Y-maze.*

mechanisms. The missing correlation between LTP and spatial memory tasks has already been demonstrated in mice lacking GluR-A (GluR1)-containing AMPA receptors (Hoffman et al., 2002; Reisel et al., 2002; Zamanillo et al., 1999). Using theta-burst stimulation (as in the current study), it was shown that the early phase of LTP in GluR-A KO mice was significantly reduced (**Figure 9**), although the maintenance phase of the LTP was *not* impaired (Hoffman et al., 2002). Considering the intact spatial reference memory and impaired spatial working memory, it was suggested that early phase LTP might take a role in spatial working memory (Reisel et al., 2002). However, in contrast to the prior hypothesis, the current study demonstrates that mice overexpressing H1aV have impaired maintenance of LTP but intact spatial reference memory. Given the spared spatial reference memory in both genotypes, we suggest that LTP maintenance, as studied using the theta burst-pairing induction protocol, is not required for this form of memory. Findings from GluR-A KOs and TgH1aV.Fb mice, however, agree that spatial working memory is impaired while early phase LTP is significantly reduced in both genotypes. Independent of the mechanistic relationship between spatial working memory and LTP, these results support the conclusion that H1aV expression impairs maintenance of LTP and temporal encoding of spatial memory.

Spatial working and reference memory tasks require multiple days of training, which might confound the observations on the functional role of an IEG. Accordingly, we also observed mice while they spontaneously explored novel and familiar objects. These observations demonstrated that the intact spatial reference memory in the Y-maze was not due to the prolonged training protocol. In agreement with a previous report (Klugmann et al., 2005), these results also showed that sustained Homer1a overexpression does not alter object recognition. Considering the intact object and spatial location perception, the observed impairment in the delayed-non-matching-to-place task cannot be due to impaired perception of space, but in contrast, reflects a genuine working memory deficit.

In TgH1aV.Fb mice expression of H1aV occurred throughout the forebrain. Among the forebrain structures, both hippocampus (e.g., Reisel et al., 2002) and prefrontal cortex (Kellendonk et al., 2006; Touzani et al., 2007) have been shown to be necessary for acquisition of working memory. To find out if H1aV expression only in hippocampus could explain the working memory deficit, we overexpressed H1aV virally in the dorsal hippocampus of adult mice. Such selective H1aV overexpression impaired the acquisition of working memory to a similar extent as transgenic forebrain expression, suggesting that the observed deficit is primarily due to Homer1a-mediated signaling in the adult dorsal hippocampus.

Taken together, our results indicate that Homer-mediated signaling in the hippocampus is required for long-term synaptic plasticity and constitutes an essential molecular pathway for encoding spatial working memory in the dorsal hippocampus.

CONFLICT OF INTEREST STATEMENT
The authors declare that research was conducted in the absence of any commercial or financial relationships that could be construed as a potential conflict of interest.

REFERENCES
Ango, F., Pin, J. -P., Tu, J. C., Xiao, B., Worley, P. F., Bockaert, J., and Fagni, L. (2000). Dendritic and axonal targeting of Type 5 metabotropic glutamate receptor Is regulated by Homer1 proteins and neuronal excitation. *J. Neurosci.* 20, 8710–8716.

Ango, F., Prezeau, L., Muller, T., Tu, J. C., Xiao, B., Worley, P. F., Pin, J. P., Bockaert, J., and Fagni, L. (2001). Agonist-independent activation of metabotropic glutamate receptors by the intracellular protein Homer. *Nature* 411, 962–965.

Baron, U., Freundlieb, S., Gossen, M., and Bujard, H. (1995). Co-regulation of two gene activities by tetracycline via a bidirectional promoter. *Nucleic Acids Res.* 23, 3605–3606.

Beneken, J., Tu, J. C., Xiao, B., Nuriya, M., Yuan, J. P., Worley, P. F., and Leahy, D. J. (2000). Structure of the Homer EVH1 domain-peptide complex reveals a new twist in polyproline recognition. *Neuron* 26, 143–154.

Bottai, D., Guzowski, J. F., Schwarz, M. K., Kang, S. H., Xiao, B., Lanahan, A., Worley, P. F., and Seeburg, P. H. (2002). Synaptic activity-induced conversion of intronic to exonic sequence in Homer 1 immediate early gene expression. *J. Neurosci.* 22, 167–175.

Brakeman, P. R., Lanahan, A. A., O'Brien, R., Roche, K., Barnes, C. A., Huganir, R. L., and Worley, P. F. (1997). Homer: a protein that selectively binds metabotropic glutamate receptors. *Nature* 386, 284–288.

Burger, C., Gorbatyuk, O. S., Velardo, M. J., Peden, C. S., Williams, P., Zolotukhin, S., Reier, P. J., Mandel, R. J., and Muzyczka, N. (2004). Recombinant AAV viral vectors pseudotyped with viral capsids from serotypes 1, 2, and 5 display differential efficiency and cell tropism after delivery to different regions of the central nervous system. *Mol. Ther.* 10, 302–317.

Cetin, A., Komai, S., Eliava, M., Seeburg, P. H., and Osten, P. (2007). Stereotaxic gene delivery in the rodent brain. *Nat. Protoc.* 1, 3166–3173.

de Bartolomeis, A., and Iasevoli, F. (2003). The Homer family and the signal transduction system at glutamatergic postsynaptic density: potential role in behavior and pharmacotherapy. *Psychopharmacol. Bull.* 37, 51–83.

Deacon, R. M., Bannerman, D. M., Kirby, B. P., Croucher, A., and Rawlins, J. N. (2002). Effects of cytotoxic hippocampal lesions in mice on a cognitive test battery. *Behav. Brain Res.* 133, 57–68.

Dittgen, T., Nimmerjahn, A., Komai, S., Licznerski, P., Waters, J., Margrie, T. W., Helmchen, F., Denk, W., Brecht, M., and Osten, P. (2004). Lentivirus-based genetic manipulations of cortical neurons and their optical and electrophysiological monitoring in vivo. *Proc. Natl. Acad. Sci. USA* 101, 18206–18211.

Duncan, R. S., Hwang, S. Y., and Koulen, P. (2005). Effects of Vesl/Homer proteins on intracellular signaling. *Exp. Biol. Med. (Maywood)* 230, 527–535.

During, M. J., Young, D., Baer, K., Lawlor, P., and Klugmann, M. (2003). Development and optimization of adeno-associated virus vector transfer into central nervous system (New Jersey, Humana press).

Francesconi, W., Cammalleri, M., and Sanna, P. P. (2004). The metabotropic glutamate receptor 5 is necessary for late-phase long-term potentiation in the hippocampal CA1 region. *Brain Res.* 1022, 12–18.

Gossen, M., and Bujard, H. (2002). Studying gene function in eukaryotes by conditional gene inactivation. *Annu. Rev. Genet.* 36, 153–173.

Gulyas, A. I., Megias, M., Emri, Z., and Freund, T. F. (1999). Total number and ratio of excitatory and inhibitory synapses converging onto single interneurons of different types in the CA1 area of the rat hippocampus. *J. Neurosci.* 19, 10082–10097.

Guzowski, J. F. (2002). Insights into immediate-early gene function in hippocampal memory consolidation using antisense oligonucleotide and fluorescent imaging approaches. *Hippocampus* 12, 86–104.

Hasan, M. T., Friedrich, R. W., Euler, T., Larkum, M. E., Giese, G., Both, M., Duebel, J., Waters, J., Bujard, H., Griesbeck, O., (2004). Functional fluorescent Ca2+ indicator proteins in transgenic mice under TET control. *PLoS Biol.* 2, e163.

Hoffman, D. A., Sprengel, R., and Sakmann, B. (2002). Molecular dissection of hippocampal theta-burst pairing potentiation. *Proc. Natl. Acad. Sci. USA* 99, 7740–7745.

Kaplitt, M. G., Leone, P., Samulski, R. J., Xiao, X., Pfaff, D. W., O'Malley, K. L., and During, M. J. (1994). Long-term gene expression and phenotypic correction using adeno-associated virus vectors in the mammalian brain. *Nat. Genet.* 8, 148–154.

Kellendonk, C., Simpson, E. H., Polan, H. J., Malleret, G., Vronskaya, S., Winiger, V., Moore, H., and Kandel, E. R. (2006). Transient and selective overexpression of dopamine D2 receptors in the striatum causes persistent abnormalities in prefrontal cortex functioning. *Neuron* 49, 603–615.

Klugmann, M., Wymond Symes, C., Leichtlein, C. B., Klaussner, B. K., Dunning, J., Fong, D., Young, D., and During, M. J. (2005). AAV-mediated hippocampal expression of short and long Homer 1 proteins differentially affect cognition and seizure activity in adult rats. *Mol. Cell. Neurosci.* 28, 347–360.

Koh, S., Chung, H., Xia, H., Mahadevia, A., and Song, Y. (2005). Environmental enrichment reverses the impaired exploratory behavior and altered gene expression induced by early-life seizures. *J. Child Neurol.* 20, 796–802.

Krestel, H. E., Shimshek, D. R., Jensen, V., Nevian, T., Kim, J., Geng, Y., Bast, T., Depaulis, A., Schonig, K., Schwenk, F., (2004). A genetic switch for epilepsy in adult mice. *J. Neurosci.* 24, 10568–10578.

Kugler, S., Lingor, P., Scholl, U., Zolotukhin, S., and Bahr, M. (2003). Differential transgene expression in brain cells in vivo and in vitro from AAV-2 vectors with small transcriptional control units. *Virology* 311, 89–95.

Kullmann, D. M., Perkel, D. J., Manabe, T., and Nicoll, R. A. (1992). Ca2+ entry via postsynaptic voltage-sensitive Ca2+ channels can transiently potentiate excitatory synaptic transmission in the hippocampus. *Neuron* 9, 1175–1183.

Lamprecht, R., and LeDoux, J. (2004). Structural plasticity and memory. *Nat. Rev. Neurosci.* 5, 45–54.

Lanahan, A., and Worley, P. (1998). Immediate-early genes and synaptic function. *Neurobiol. Learn. Mem.* 70, 37–43.

Mack, V., Burnashev, N., Kaiser, K. M., Rozov, A., Jensen, V., Hvalby, O., Seeburg, P. H., Sakmann, B., and Sprengel, R. (2001). Conditional restoration of hippocampal synaptic potentiation in Glur-A-deficient mice. *Science* 292, 2501–2504.

Mastakov, M. Y., Baer, K., Symes, C. W., Leichtlein, C. B., Kotin, R. M., and During, M. J. (2002). Immunological aspects of recombinant adeno-associated virus delivery to the mammalian brain. *J. Virol.* 76, 8446–8454.

Mayford, M., Bach, M. E., Huang, Y. Y., Wang, L., Hawkins, R. D., and Kandel, E. R. (1996). Control of memory formation through regulated expression of a CaMKII transgene. *Science* 274, 1678–1683.

Miyoshi, H., Blomer, U., Takahashi, M., Gage, F. H., and Verma, I. M. (1998). Development of a self-inactivating lentivirus vector. *J. Virol.* 72, 8150–8157.

Nagai, T., Ibata, K., Park, E. S., Kubota, M., Mikoshiba, K., and Miyawaki, A. (2002). A variant of yellow fluorescent protein with fast and efficient maturation for cell-biological applications. *Nat. Biotechnol.* 20, 87–90.

Naisbitt, S., Kim, E., Tu, J. C., Xiao, B., Sala, C., Valtschanoff, J., Weinberg, R. J., Worley, P. F., and Sheng, M. (1999). Shank, a novel family of postsynaptic density proteins that binds to the NMDA receptor/PSD-95/GKAP complex and cortactin. *Neuron* 23, 569–582.

Nelson, S. E., Duricka, D. L., Campbell, K., Churchill, L., and Krueger, J. M. (2004). Homer1a and 1bc levels in the rat somatosensory cortex vary with the time of day and sleep loss. *Neurosci. Lett.* 367, 105–108.

Pastalkova, E., Serrano, P., Pinkhasova, D., Wallace, E., Fenton, A. A., and Sacktor, T. C. (2006). Storage of Spatial Information by the Maintenance Mechanism of LTP. *Science* 313, 1141–1144.

Peel, A. L., Zolotukhin, S., Schrimsher, G. W., Muzyczka, N., and Reier, P. J. (1997). Efficient transduction of green fluorescent protein in spinal cord neurons using adeno-associated virus vectors containing cell type-specific promoters. *Gene. Ther.* 4, 16–24.

Reisel, D., Bannerman, D. M., Schmitt, W. B., Deacon, R. M., Flint, J., Borchardt, T., Seeburg, P. H., and Rawlins, J. N. (2002). Spatial memory dissociations in mice lacking GluR1. *Nat. Neurosci.* 5, 868–873.

Richichi, C., Lin, E. J., Stefanin, D., Colella, D., Ravizza, T., Grignaschi, G., Veglianese, P., Sperk, G., During, M. J., and Vezzani, A. (2004). Anticonvulsant and antiepileptogenic effects mediated by adeno-associated virus vector neuropeptide Y expression in the rat hippocampus. *J. Neurosci.* 24, 3051–3059.

Sala, C., Piech, V., Wilson, N. R., Passafaro, M., Liu, G., and Sheng, M. (2001). Regulation of dendritic spine morphology and synaptic function by Shank and Homer. *Neuron* 31, 115–130.

Schmitt, W. B., Sprengel, R., Mack, V., Draft, R. W., Seeburg, P. H., Deacon, R. M., Rawlins, J. N., and Bannerman, D. M. (2005). Restoration of spatial working memory by genetic rescue of GluR-A-deficient mice. *Nat. Neurosci.* 8, 270–272.

Schonig, K., and Bujard, H. (2003). Generating conditional mouse mutants via tetracycline-controlled gene expression. *Methods Mol. Biol.* 209, 69–104.

Sheng, M., and Greenberg, M. E. (1990). The regulation and function of c-fos and other immediate early genes in the nervous system. *Neuron* 4, 477–485.

Shevtsova, Z., Malik, J. M., Michel, U., Bahr, M., and Kugler, S. (2005). Promoters and serotypes: targeting of adeno-associated virus vectors for gene transfer in the rat central nervous system in vitro and in vivo. *Exp. Physiol.* 90, 53–59.

Stupien, G., Florian, C., and Roullet, P. (2003). Involvement of the hippocampal CA3-region in acquisition and in memory consolidation of spatial but not in object information in mice. *Neurobiol. Learn. Mem.* 80, 32–41.

Thinus-Blanc, C., Save, E., Rossi-Arnaud, C., Tozzi, A., and Ammassari-Teule, M. (1996). The differences shown by C57BL/6 and DBA/2 inbred mice in detecting spatial novelty are subserved by a different hippocampal and parietal cortex interplay. *Behav. Brain. Res.* 80, 33–40.

Touzani, K., Puthanveettil, S. V., and Kandel, E. R. (2007). Consolidation of learning strategies during spatial working memory task requires protein synthesis in the prefrontal cortex. *PNAS* 104, 5632–5637.

Tu, J. C., Xiao, B., Naisbitt, S., Yuan, J. P., Petralia, R. S., Brakeman, P., Doan, A., Aakalu, V. K., Lanahan, A. A., Sheng, M., and Worley, P. F. (1999). Coupling of mGluR/Homer and PSD-95 complexes by the Shank family of postsynaptic density proteins. *Neuron* 23, 583–592.

Tu, J. C., Xiao, B., Yuan, J. P., Lanahan, A. A., Leoffert, K., Li, M., Linden, D. J., and Worley, P. F. (1998). Homer binds a novel proline-rich motif and links group 1 metabotropic glutamate receptors with IP3 receptors. *Neuron* 21, 717–726.

Van Keuren-Jensen, K., and Cline, H. T. (2006). Visual Experience Regulates Metabotropic Glutamate Receptor-Mediated Plasticity of AMPA Receptor Synaptic Transmission by Homer1a Induction. *J. Neurosci.* 26, 7575–7580.

Vazdarjanova, A., and Guzowski, J. F. (2004). Differences in hippocampal neuronal population responses to modifications of an environmental context: evidence for distinct, yet complementary, functions of CA3 and CA1 ensembles. *J. Neurosci.* 24, 6489–6496.

Vazdarjanova, A., McNaughton, B. L., Barnes, C. A., Worley, P. F., and Guzowski, J. F. (2002). Experience-dependent coincident expression of the effector immediate-early genes arc and Homer 1a in hippocampal and neocortical neuronal networks. *J. Neurosci.* 22, 10067–10071.

Whitlock, J. R., Heynen, A. J., Shuler, M. G., and Bear, M. F. (2006). Learning Induces Long-Term Potentiation in the Hippocampus. *Science* 313, 1093–1097.

Xiao, B., Tu, J. C., and Worley, P. F. (2000). Homer: a link between neural activity and glutamate receptor function. *Curr. Opin. Neurobiol.* 10, 370–374.

Xu, R., Janson, C. G., Mastakov, M., Lawlor, P., Young, D., Mouravlev, A., Fitzsimons, H., Choi, K. L., Ma, H., Dragunow, M., *et al.* (2001). Quantitative comparison of expression with adeno-associated virus (AAV-2) brain-specific gene cassettes. *Gene. Ther.* 8, 1323–1332.

Zamanillo, D., Sprengel, R., Hvalby, O., Jensen, V., Burnashev, N., Rozov, A., Kaiser, K. M., Koster, H. J., Borchardt, T., Worley, P., *et al.* (1999). Importance of AMPA receptors for hippocampal synaptic plasticity but not for spatial learning. *Science* 284, 1805–1811.

Zola, S. M., Squire, L. R., Teng, E., Stefanacci, L., Buffalo, E. A., and Clark, R. E. (2000). Impaired recognition memory in monkeys after damage limited to the hippocampal region. *J. Neurosci.* 20, 451–463.